MJFAS
Malaysian Journal of Fundamental and Applied Sciences

REVIEW ARTICLE

Finite Element Analysis of Biomagnetic Fluid Flow in a Channel with an Overlapping Stenosis

Normazni Abdullah, Zuhaila Ismail*

Department of Mathematical Sciences, Faculty of Science, Universiti Teknologi Malaysia, 81310 UTM Johor Bahru, Johor, Malaysia

Abstract Analysis of biomagnetic fluid (blood) flow (BFD) is important due to the potential biomedical applications that have been proposed such as cell separation for magnetic devices, drug delivery using magnetic particles for the treatment of cancer tumours, hyperthermia, and the reduction of bleeding during surgeries. In this study, the effects of spatially varying magnetic field on a straight channel with an overlapping stenosis is investigated numerically using finite element method (FEM). The mathematical model of biomagnetic fluid is constructed based on the coupled study of Navier-Stokes equations with the principles of ferrohydrodynamic (FHD). While the flow in a constricted artery is considered to be Newtonian, steady, two-dimensional and isothermal. Galerkin finite element method is used to discretize the governing equations and then the source code is developed by using MATLAB software. The source code is validated, and the results is compared with the previous literature. Based on the findings, the introduction of magnetic field alters the behaviour of blood flow in the area near the magnetic source. The increment of magnetic field intensity near stenosis area causes the recirculation area downstream to become smaller. This could be seen from the velocity profile and streamline pattern of constricted artery.

Keywords: FEM, BFD, overlapping stenosis, blood flow.

Introduction

Cardiovascular complications involve the disorder of the heart and blood vessels [1] and may lead to fatalities [2]. Some of the examples of cardiovascular disease are coronary heart disease, cerebrovascular disease and peripheral arterial disease. Coronary heart disease occurred due to atherosclerosis which is the hardening of arterial wall forming a stenosis or plaque. As a result, it causes the constriction in the artery and limit the blood supply demands [3]. Abnormality such as stenosis in blood vessels highly influenced the hemodynamic of flow [4]. In recent years, biomagnetic fluid flow (BFD) has become an active area of study due to the advancement of its application in bioengineering and medicine [5]. Some of the applications in bioengineering and medicine applying the concept of magnetic field on the flow of biofluids are the development of magnetic devices such as magnetic drug targeting and magnetic cell separation [6]. Blood typically known as the most common biofluid due to the special characteristics it possessed [7-10]. It is revealed that the red blood cells able to orientate in the presence of magnetic field [11] and the orientation state depends on the state of hemoglobin [12]. Blood magnetization properties is affected by the concentration of oxygen where it possesses the diamagnetic and paramagnetic properties as they become oxygenated and deoxygenated respectively [13].

***For correspondence:**
zuhaila@utm.my

Received: 30 Sept. 2021
Accepted: 26 Dec. 2022

There are several mathematical models proposed for BFD [14]. It is based on the modified Stokes principles with the assumption that the fluid behaviour is also a function of magnetization. Based on the developed model, it is governed mainly by the principle of magnetohydrodynamics (MHD) and ferrohydrodynamic (FHD). Magnetohydrodynamics is a couple study between fluid dynamics and electromagnetism comprises of the Navier Stokes and Maxwell's equations. While for ferrohydrodynamic, the presence of magnetic field causes the magnetic fluid to undergo polarization and hence induces the magnetization force inside the fluid [15].

To obtain the numerical solution of the mathematical model, finite element method (FEM) will be used. Within few decades, numerical technique has evolved from applications in structural engineering to most of computational approach for science and technology areas [16-17]. A finite element Taylor-Galerkin scheme with operator splitting methods was presented by Formaggia *et al*. [18]. Moreover, Sousa *et al*. [19] also considered the FEM to solve the Navier-Stokes equations in her study. They implement the streamline Petrov Galerkin method in order to eliminate the stability problem. Wei *et al*. [20] used the FEM for cardiac blood flow simulation with echo where it allows data to be assimilated in a very flexible manner so that accurate measurements are more closely matched with the numerical solution than less accurate data. Zain *et al*. [21] study on steady state flow of blood in bifurcated artery by considering the blood as generalized Newtonian fluid. Simulation is performed by implemented Taylor-Galerkin finite element as a mothod of solution. Achab *et al*. [22] investigate the periodic blood flow through a stenotic artery by considering the Cross model and generalised power law as the shear thinning characteristic. They introducing the penalty function method following the standard Galerkin approach to eliminate the term of pressure that arises in the equation of motion. Bazilevs *et al*. [23] conducted an analysis of isogeometric blood flow by NURBS-based approaches. They constructed a realistic geometry by patient-specific vascular geometry and solve the problem by using FEM. They conclude that the FEM provide significant benefit for analysis where the mesh allows to refine the boundary layer and crucial for obtaining accurate wall quantities such as wall shear stress. FEM is proven to provide the researcher with an accurate result after it has been validated with the experimental results and it comprises of various types such as Generalized Finite Element method, Galerkin method and applied element method.

To the best of the author's knowledge, there were none of the studies on BFD flow in a straight arterial channel in the presence of overlapping stenosis were addressed in the literature. Hence, in the present study, the main objective is to develop a model of BFD flow in a straight arterial channel in the presence of overlapping stenosis and to solve and investigate it numerically using FEM. This study considered the flow to be steady, isothermal, two-dimensional and laminar. The solution of the problem is obtained numerically by discretizing the governing equations using finite element Galerkin weighted residual method. Mixed formulation of finite element method is used to discretize the problem due to its stability and cost effective. MATLAB coding is then developed based on this formulation to obtain the required solution.

Mathematical Formulation

The fluid flow model is based on the Newtonian Navier-Stokes equations where the blood flow is assumed to be two-dimensional, steady and laminar; a fluid that travels smoothly in regular paths. In addition to that, the fluid is flowing under the presence of magnetic field since this study focus on biomagnetic fluid flow in a channel artery. The flow is isothermal where temperature changes are negligible and the magnetic field involves are based on the force arising due to spatially varying magnetic field (magnetic gradient). Thus, the governing equations for this biomagnetic fluid flow problem is as stated below

$$\bar{\rho}\left(\bar{u}\frac{\partial\bar{u}}{\partial\bar{x}}+\bar{v}\frac{\partial\bar{u}}{\partial\bar{y}}\right)=-\frac{\partial\bar{p}}{\partial\bar{x}}+\bar{\mu}\left(\frac{\partial^2\bar{u}}{\partial\bar{x}^2}+\frac{\partial^2\bar{u}}{\partial\bar{y}^2}\right)+\bar{\mu}_0\bar{M}\frac{\partial\bar{H}}{\partial\bar{x}}, \tag{1}$$

$$\bar{\rho}\left(\bar{u}\frac{\partial\bar{v}}{\partial\bar{x}}+\bar{v}\frac{\partial\bar{v}}{\partial\bar{y}}\right)=-\frac{\partial\bar{p}}{\partial\bar{y}}+\bar{\mu}\left(\frac{\partial^2\bar{v}}{\partial\bar{x}^2}+\frac{\partial^2\bar{v}}{\partial\bar{y}^2}\right)+\bar{\mu}_0\bar{M}\frac{\partial\bar{H}}{\partial\bar{y}}, \tag{2}$$

$$\frac{\partial\bar{u}}{\partial\bar{x}}+\frac{\partial\bar{v}}{\partial\bar{y}}=0. \tag{3}$$

In the above equations, $\bar{u}$ and $\bar{v}$ are the dimensional velocity, $\bar{p}$ is the pressure, $\bar{\rho}$ is the density of fluid, $\bar{\mu}$ is the dynamic viscosity, $\bar{\mu}_0$ is the magnetic permeability of vacuum, $\bar{M}$ is the magnetization, $\bar{H}=\left(\bar{H}_x,\bar{H}_y\right)$ is the magnetic field strength and $\bar{\sigma}$ is the electrical conductivity. The terms $\bar{\mu}_0\bar{M}\frac{\partial\bar{H}}{\partial\bar{x}}$ and $\bar{\mu}_0\bar{M}\frac{\partial\bar{H}}{\partial\bar{y}}$ represent the components of magnetic force per unit volume and well known for FHD term. Here, μ_0 is the magnetic permeability of vacuum or free space while μ_r is the relative magnetic permeability. The magnetization equations is $\bar{M}=\bar{\chi}\bar{H}$ where $\bar{\chi}$ is magnetic susceptibility. For blood, its magnetic susceptibility depends on the oxygenation state of the blood which are -6.6×10^{-7} and 3.5×10^{-6} for oxygenated and deoxygenated blood respectively. The components of magnetic field intensity, $\bar{H}_x$ and $\bar{H}_y$ along the $\bar{x}$ and $\bar{y}$ coordinates are given according to [6] as

$$\bar{H}_x=\frac{\gamma}{2\pi}\frac{\bar{y}-\bar{b}}{\left(\bar{x}-\bar{a}\right)^2+\left(\bar{y}-\bar{b}\right)^2}, \tag{4}$$

$$\bar{H}_y=-\frac{\gamma}{2\pi}\frac{\bar{x}-\bar{a}}{\left(\bar{x}-\bar{a}\right)^2+\left(\bar{y}-\bar{b}\right)^2}. \tag{5}$$

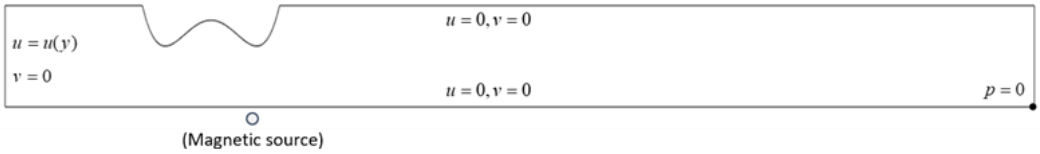

Figure 1. Geometry of artery for straight rectangular channel with an overlapping stenosis.

In this straight rectangular channel problem (see Figure 1), a spatially varying magnetic field is generated by placing the magnetic source directly below the bottom wall of stenosis formation at $(x,y)=(3.8,-0.01)$. The velocity profile near the entrance is assumed to be fully developed while no-slip condition is assumed for the upper and lower walls. Traction free condition is set as zero for the outflow with the pressure point constraint, $\bar{p}=0$ being implemented at $(\bar{L},0)$. The boundary conditions for the channel can be expressed mathematically as

$$\begin{aligned}
&\text{Inlet} && \left(\bar{x}=0,\ 0\le\bar{y}\le\bar{h}\right):\bar{u}=\bar{u}\left(\bar{y}\right),\ \bar{v}=0,\\
&\text{Upper wall} && \left(\bar{y}=0,\ 0\le\bar{x}\le\bar{L}\right):\bar{u}=0,\ \bar{v}=0,\\
&\text{Lower wall} && \left(\bar{x}=\bar{L},\ 0\le\bar{y}\le\bar{h}\right):\bar{u}=0,\ \bar{v}=0.
\end{aligned} \tag{6}$$

where *h* is the height of artery and L is the length of artery.

Galerkin Weighted Residual Method

The differential equations in Equation (1) - (5) together with the boundary conditions as stated in Equation (6) are now transform into dimensionless form by substituting the dimensionless variables given below.

$$x=\frac{\bar{x}}{\bar{h}},\ y=\frac{\bar{y}}{\bar{h}},\ u=\frac{\bar{u}}{\bar{u}_r},\ v=\frac{\bar{v}}{\bar{u}_r},\ p=\frac{\bar{p}}{\bar{\rho}\bar{u}_r^{\,2}},\ H_x=\frac{\bar{H}_x}{\bar{H}_0},\ H_y=\frac{\bar{H}_y}{\bar{H}_0},$$

where $\bar{H}_0=\bar{H}_0\left(\bar{a},0\right)$ is the reference magnetic field intensity, $\bar{h}$ is the reference length between two plates at the entrance and $\bar{u}_r$ is maximum velocity of the blood at the inlet.

The dimensionless equations for Equations (1) – (3) are obtained as follow

$$u\frac{\partial u}{\partial x}+v\frac{\partial u}{\partial y}=-\frac{\partial p}{\partial x}+\frac{1}{\mathrm{Re}}\left(\frac{\partial^2 u}{\partial x^2}+\frac{\partial^2 u}{\partial y^2}\right)+Mn_F H\frac{\partial H}{\partial x}, \tag{7}$$

$$u\frac{\partial v}{\partial x}+v\frac{\partial v}{\partial y}=-\frac{\partial p}{\partial y}+\frac{1}{\mathrm{Re}}\left(\frac{\partial^2 v}{\partial x^2}+\frac{\partial^2 v}{\partial y^2}\right)+Mn_F H\frac{\partial H}{\partial y}, \tag{8}$$

$$\frac{\partial u}{\partial x}+\frac{\partial v}{\partial y}=0. \tag{9}$$

The dimensionless form of the magnetic field intensity, $H=\left(H_x,H_y\right)$ and the boundary conditions, refer Equations (4) – (6) are given as follow

$$H_x=\frac{|-b|\left(b-y\right)}{\left(x-a\right)^2+\left(y-b\right)^2}, \tag{10}$$

$$H_y=\frac{-|-b|\left(x-a\right)}{\left(x-a\right)^2+\left(y-b\right)^2}, \tag{11}$$

Inlet $\left(x=0,\ 0\le y\le 1\right):u=u\left(y\right),\ v=0,$

Upper wall $\left(y=0,\ 0\le x\le L/h\right):u=0,\ v=0,$

Lower wall $\left(x=L/h,\ 0\le y\le 1\right):u=0,\ v=0.$ (12)

The non-dimensional parameters entering now into the problem under consideration are

Reynolds number: $$\mathrm{Re}=\frac{\bar{h}\bar{\rho}\bar{u}_r}{\bar{\mu}}. \tag{13}$$

Magnetic number due FHD $$Mn_F=\frac{\bar{\mu}_0\bar{\chi}\bar{H}_0^{\,2}}{\bar{\rho}\bar{u}_r^{\,2}}. \tag{14}$$

Then, the dimensionless equations in Equations (6) – (11) are discretized by using Galerkin weighted residual method to obtain a system of algebraic equation. The discretization process is to interpolate the velocity function u , v and pressure p by using the unstructured triangular elements. The variables $\left(u^{e_i},v^{e_i},p^{e_i}\right)$ are approximated for quadratic shape function, $N_j^{\,e_i}\left(x,y\right)$ and linear shape function,

$L_k^{e_i}(x,y)$ as

$$\begin{aligned} u^{e_i}(x,y) &= N_j^{e_i}(x,y)u_j^{e_i}, \\ v^{e_i}(x,y) &= N_j^{e_i}(x,y)v_j^{e_i}, \\ p^{e_i}(x,y) &= L_k^{e_i}(x,y)\,p_k^{e_i}. \quad j=1,2,3,...,6 \text{ and } k=1,2,3 \end{aligned} \tag{15}$$

where e_i denote the finite element at $i=1,2,3,...,n$. While the weighting function, $w(x,y)$ for momentum and continuity equations is given respectively by

$$\begin{aligned} w_l(x,y) &= N_l^{e_i}(x,y), \\ w_m(x,y) &= L_m^{e_i}(x,y). \quad l=1,2,3,...,6 \text{ and } m=1,2,3 \end{aligned} \tag{16}$$

The next step is to distribute the differentiation by applying the integration by parts for the second order derivatives terms along with the divergence theorem. Then, by using the Green's theorem, the boundary conditions (12) associated with the differential equations (6) – (11) which are natural and essential boundary condition is induced. The resulting equations obtained are

$$\int_\Omega \left\{ \begin{array}{l} N_l^{e_i}\left(u^{e_i}\dfrac{\partial u^{e_i}}{\partial x}+v\dfrac{\partial u^{e_i}}{\partial y}\right)+N_l^{e_i}\dfrac{\partial p^{e_i}}{\partial x}+\dfrac{1}{\mathrm{Re}}\left[\dfrac{\partial N_l^{e_i}}{\partial x}\dfrac{\partial u^{e_i}}{\partial x}+\dfrac{\partial N_l^{e_i}}{\partial y}\dfrac{\partial u^{e_i}}{\partial y}\right] \\ -Mn_F N_l^{e_i} H\dfrac{\partial H}{\partial x} \end{array} \right\} d\Omega = B_{cx} \tag{17}$$

$$\int_\Omega \left\{ \begin{array}{l} N_l^{e_i}\left(u^{e_i}\dfrac{\partial v^{e_i}}{\partial x}+v\dfrac{\partial v^{e_i}}{\partial y}\right)+N_l^{e_i}\dfrac{\partial p^{e_i}}{\partial y}+\dfrac{1}{\mathrm{Re}}\left[\dfrac{\partial N_l^{e_i}}{\partial x}\dfrac{\partial v^{e_i}}{\partial x}+\dfrac{\partial N_l^{e_i}}{\partial y}\dfrac{\partial v^{e_i}}{\partial y}\right] \\ -Mn_F N_l^{e_i} HS\dfrac{\partial H}{\partial y} \end{array} \right\} d\Omega = B_{cy} \tag{18}$$

where B_{cx} and B_{cy} are

$$\begin{aligned} B_{cx} &= -\int_\Gamma \left\{ \frac{1}{\mathrm{Re}}\left[N_l^{e_i}\frac{\partial u^{e_i}}{\partial x}n_x + N_l^{e_i}\frac{\partial u^{e_i}}{\partial y}n_y \right] \right\} d\Gamma, \\ B_{cy} &= -\int_\Gamma \left\{ \frac{1}{\mathrm{Re}}\left[N_l^{e_i}\frac{\partial v^{e_i}}{\partial x}n_x + N_l^{e_i}\frac{\partial v^{e_i}}{\partial y}n_y \right] \right\} d\Gamma. \end{aligned} \tag{19}$$

Since traction free condition is considered in this study, the term on the right-hand side of Equations (17) and (18) are zero and Equation (19) can be written as

$$B_{cx}=0, B_{cy}=0.$$

Finally, substitute the approximate solution as defined in Equation (15) to obtain the element equations as written in matrix form as below

$$\begin{bmatrix} k_{11} & 0 & k_{13} \\ 0 & k_{22} & k_{23} \\ k_{31} & k_{32} & 0 \end{bmatrix} \begin{Bmatrix} \{u_j^{e_1}\}^T \\ \{v_j^{e_1}\}^T \\ \{p_k^{e_1}\}^T \end{Bmatrix} = \begin{bmatrix} r_1 \\ r_2 \\ 0 \end{bmatrix} \tag{20}$$

where

$$k_{11}=\int_{\Omega}\left\{\begin{array}{l}\left\{N_l^{e_i}\right\}\left(u^{e_i}\dfrac{\partial\left\{N_j^{e_i}\right\}}{\partial x}+v^{e_i}\dfrac{\partial\left\{N_j^{e_i}\right\}}{\partial y}\right)\\ +\dfrac{1}{\mathrm{Re}}\left(\dfrac{\partial\left\{N_l^{e_i}\right\}}{\partial x}\dfrac{\partial\left\{N_j^{e_i}\right\}}{\partial x}+\dfrac{\partial\left\{N_l^{e_i}\right\}}{\partial y}\dfrac{\partial\left\{N_j^{e_i}\right\}}{\partial y}\right)\end{array}\right\}d\Omega,\ k_{13}=\int_{\Omega}\left\{N_l^{e_i}\right\}\frac{\partial\left\{L_k^{e_i}\right\}}{\partial x}d\Omega$$

$$k_{22}=\int_{\Omega}\left\{\begin{array}{l}\left\{N_l^{e_i}\right\}\left(u^{e_i}\dfrac{\partial\left\{N_j^{e_i}\right\}}{\partial x}+v^{e_i}\dfrac{\partial\left\{N_j^{e_i}\right\}}{\partial y}\right)\\ +\dfrac{1}{\mathrm{Re}}\left[\dfrac{\partial\left\{N_l^{e_i}\right\}}{\partial x}\dfrac{\partial\left\{N_j^{e_i}\right\}}{\partial x}+\dfrac{\partial\left\{N_l^{e_i}\right\}}{\partial y}\dfrac{\partial\left\{N_j^{e_i}\right\}}{\partial y}\right]\end{array}\right\}d\Omega,\ k_{23}=\int_{\Omega}\left\{N_l^{e_i}\right\}\frac{\partial\left\{L_k^{e_i}\right\}}{\partial y}d\Omega$$

$$k_{31}=\int_{\Omega}\left\{L_m^{e_i}\right\}\frac{\partial\left\{N_j^{e_i}\right\}}{\partial x}d\Omega,\ k_{32}=\int_{\Omega}\left\{L_m^{e_i}\right\}\frac{\partial\left\{N_j^{e_i}\right\}}{\partial y}d\Omega,$$

$$r_1=Mn_F\int_{\Omega}\left\{N_l^{e_i}\right\}H\frac{\partial H}{\partial x}d\Omega,\ r_2=Mn_F\int_{\Omega}\left\{N_l^{e_i}\right\}H\frac{\partial H}{\partial y}d\Omega.$$

Equation (20) is called the local element matrix. The matrices need to be assembled into global matrix first in order to solve it. Since the equation is nonlinear in nature, the matrix is then solved by using Newton-Raphson method.

Model Validation

The source code for the formulation is developed using MATLAB software. Verification against benchmark is conducted to ensure the source code is reliable and functioning properly. Note that, Lorentz force, N will not be considered in this formulation. This is because, Lorentz force will not have any significant effect on the flow field due to the presence of high magnetic field gradient as in spatially varying magentic field. Hence, $N=0$. The density and dynamic viscosity of blood is $p=1050\mathrm{kgm}^{-3}$ and $\mu=3.2\times10^{-3}\mathrm{kgm}^{-1}\mathrm{s}^{-1}$ respectively. The computational domain consists of a square cavity with the side lengths of $0.05\mathrm{m}$. The top lid is moving with a horizontal velocity of $\overline{u}_r=2.438\times10^{-2}\mathrm{ms}^{-1}$ in the positive $x-$ direction. The magnetic source is applied close to the bottom center of the domain as shown in Figure 2. Figure 2 shows contour lines of the spatially varying magnetic field that will be considered in this model validation.

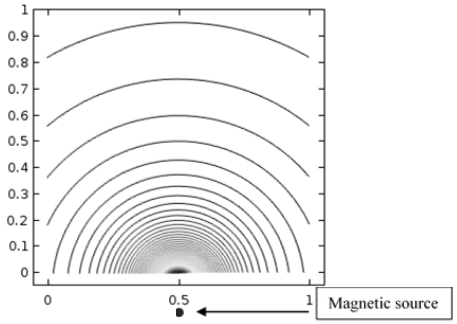

Figure 2. Contour lines of the dimensionless spatially varying magnetic field.

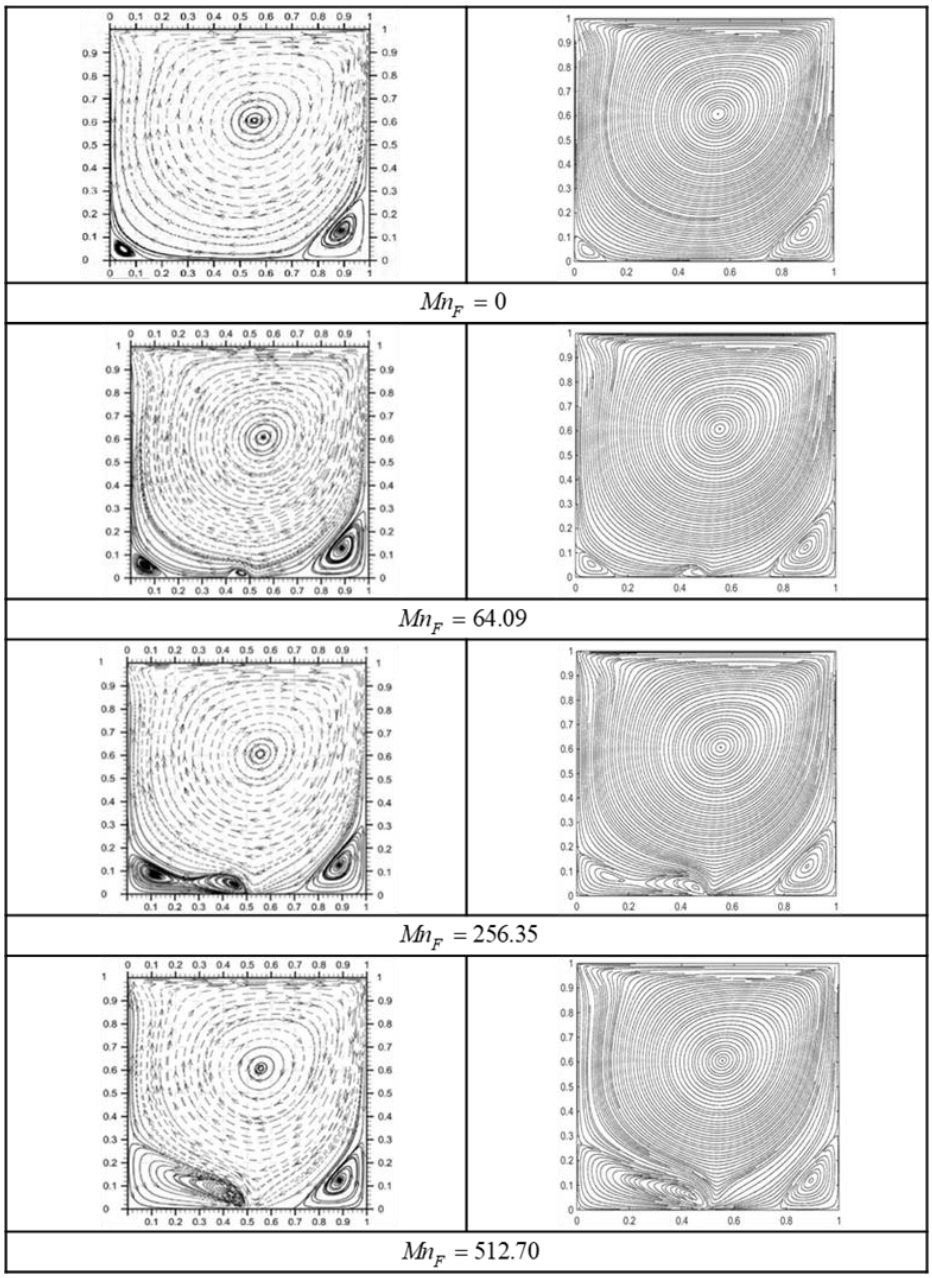

Figure 3. Streamlines for $\mathrm{Re} = 400$ for various magnetic field strength between finite difference method [24] (left) and current study, Galerkin finite element method (right).

The model is validate using previous literature from [24] and the results shows a good agreement for both the numerical method used. Figure 3 shows the streamline pattern of lid driven cavity for ferrohydrodynamics case as compared between finite difference method by Tzirtzilakis and Xenos [24] and Galerkin finite element method from the current study, Abdullah *et al*. [25].

Results and Discussion

The developed source code for BFD case which had been validated with the benchmark problem in the previous section Model validation is modified to obtain the numerical results for overlapping stenosis in a straight artery channel.

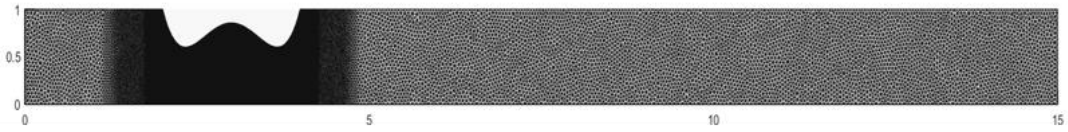

Figure 4. Mesh of the geometry of artery for straight rectangular channel with an overlapping stenosis.

The problem domain and boundary conditions for straight channel is shown in Figure 1. Mesh test is conducted to ensure that the results is not mesh dependent. Noted that the maximum point stated in Table 1 is refer to the maximum velocity. In finite element formulation, it is compulsory to mesh the problem domain. The domain in this study is discretized into unstructured triangular element as shown in Figure 4 and the mesh will be set to be denser at the area of magnetic source since the effect of magnetic field will be expected to show a characteristics behaviour here. The computed results of the discretized domain can be seen in Table 1.

Table 1. Mesh test result.

Mesh	Number of Elements	Number of Nodes	Degree of Freedom	Maximum point
1.	14762	7742	30251	1.5202
2.	19046	9913	38871	1.543
3.	25138	13008	51153	1.5364
4.	34721	17851	70422	1.5207
5.	39028	20020	79067	1.558

Based on the Figure 5, the result shown that the axial velocity is almost equivalent for each of the computed mesh. Thus, it can be concluded that the results are not dependent on the mesh or the total number of elements. Hence, Mesh 3 is chosen to get an excellent solution considering more time is needed for computation if mesh with too many numbers of element is selected. In this formulation, the fluid is considered as blood flowing in artery with the presence of overlapping stenosis. The parameter for the blood is the same as presented by Kasiman [5] with the density of 1050 kg/m^3 and viscosity of $3.2x10^{-3}$ kgm/ms. The velocity contour and streamline patterns results obtained for the effect of different magnetic field on channel with stenosis is presented in Figure 6.

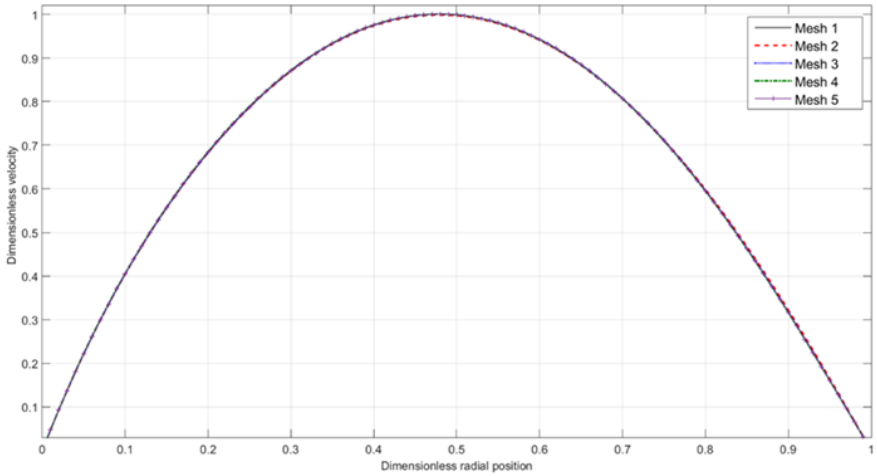

Figure 5. The dimensionless axial velocity for different mesh at $x = 1$ with $\mathrm{Re} = 250$ and $Mn_F = 0$.

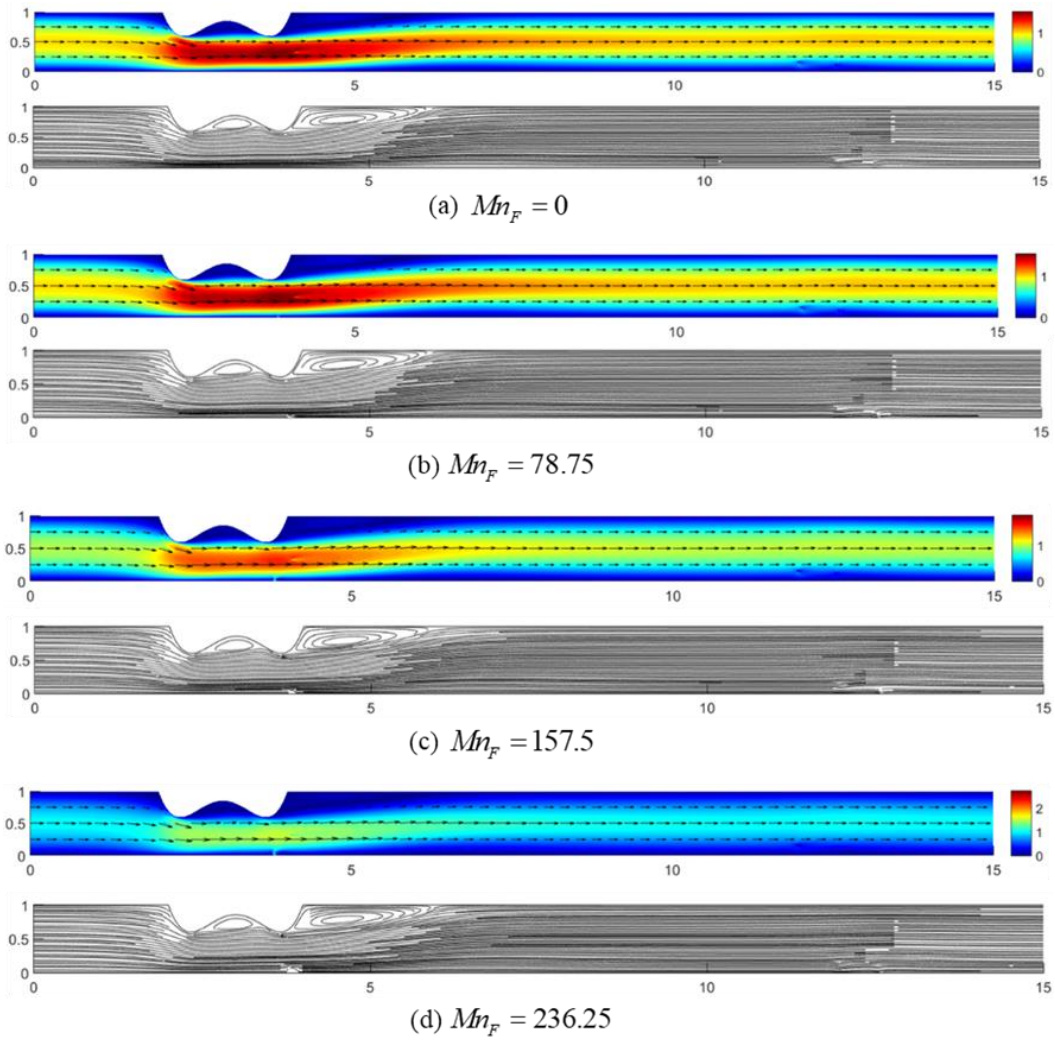

Figure 6. Velocity contour and streamlines pattern for biomagnetic fluid flow with an overlapping stenosis for $\mathrm{Re} = 250$ at different magnetic number for $Mn_F = 0,\ 78.75,\ 157.5$ and 236.25.

The velocity contour and streamline patterns in Figure 6 show that when the magnetic source is introduced to the flow, there exist a formation of small vortex near the magnetic source. The magnetic intensity is increase from $78.75,\ 157.5$ and 236.25 and it can be seen from the streamline patterns that the vortex near magnetic source increase in size as the magnetic intensity is increased. For velocity contour, the velocity distribution along the channel shows a significant change as the magnetic source is introduced. This can be seen clearly from Figure 7 below for axial velocity profile before the magnetic source is introduced, at the magnetic field source and after the magnetic source at $x = 3.0,\ 3.8$ and 5.0 respectively.

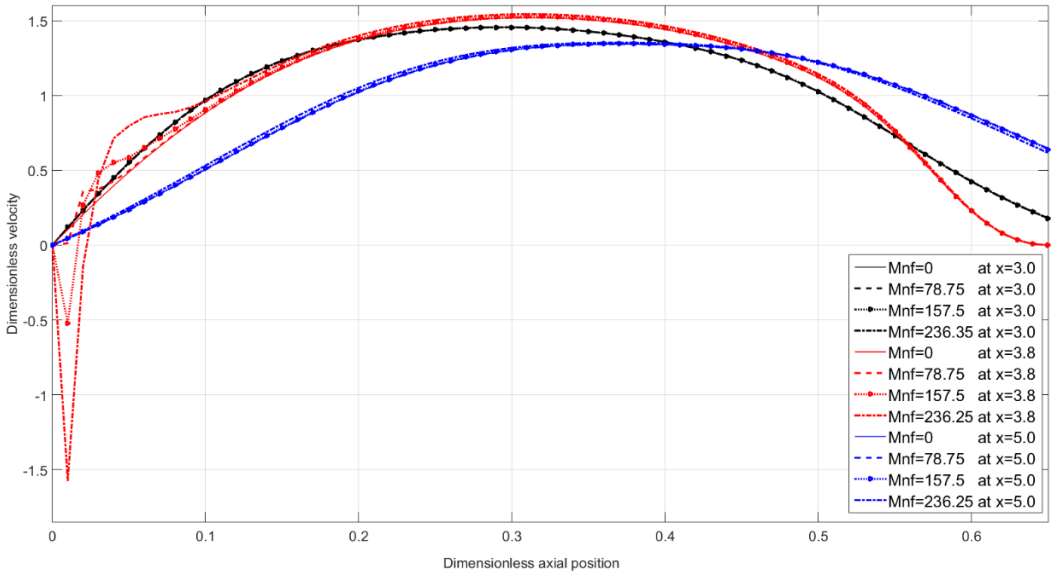

Figure 7. Variation of Axial Velocity at Different Magnetic Field Intensity $Mn_F = 0,\ 78.75,\ 157.5$ and 236.25 for $x = 3.0,\ 3.8$ and 5.0 with $\mathrm{Re} = 250$.

Figure 7 shows that x at 3.0 denoted the variation of axial velocity before magnetic source is introduced and at $x = 3.8$ the magnetic source is located. It can be observed that there is substantial change on the velocity profile as the magnetic intensity increased. The velocity flow change from negative to positive range which shows the existence of circulation zone as the magnetic field gradient is imposed. The effects of the circulation zone can be seen at $x = 5.0$. Although the change of velocity is not significant, it can be still observed that as the magnetic intensity is increased, the velocity profile shows slight decrement at the upper wall as compared to flow without magnetic intensity.

The comparison of axial velocity along the channel at $y = 0.01$ is presented in Figure 8. At the inlet of the channel, the axial velocity is increasing continuously as it flows through the first throat of the overlapping stenosis. This is due to the action of the fluid to compressed itself in order to flow into the constricted channel. Then, velocity continue to drop as it passes through the stenosis until it reaches the magnetic source. As the magnetic field is introduced at the second throat of stenosis, at $x = 3.8$ the flow reaches its maximum velocity at the highest magnetic intensity of $Mn_F = 232.25$. Then, the flow drops again after it passes through the magnetic source and after that the flow regain their inlet profiles as it moves downstream the channel. Based on Figure 8, it can be concluded that the application of magnetic field affected the maximum velocity of the flow since it changes from inside the stenosis constriction to the magnetic source location instead.

Conclusions

The geometry of straight channel artery with an overlapping stenosis in the presence of magnetic field was solved by introducing Galerkin weighed residual based on finite element method. It can be concluded that, when the magnetic field was introduced to the flow, there exist a circulation zone near the magnetic source and the circulation increases as the magnetic field intensity is increased. However, for the recirculation zones near the stenosis upstream, as the magnetic intensity increase, the circulation zones shrink. This indicates that the applications of magnetic field influenced the flow of blood. In addition to that, the results also demonstrated the use of FEM in solving complex geometry. For future study, author would like to suggest for the improvement on the mathematical model by the addition of heat and mass transfer. The inclusion of heat and mass in the study of biomagnetic fluid flow is necessary since heat transfer occurs in the natural environment, in engineering equipments and in living creature.

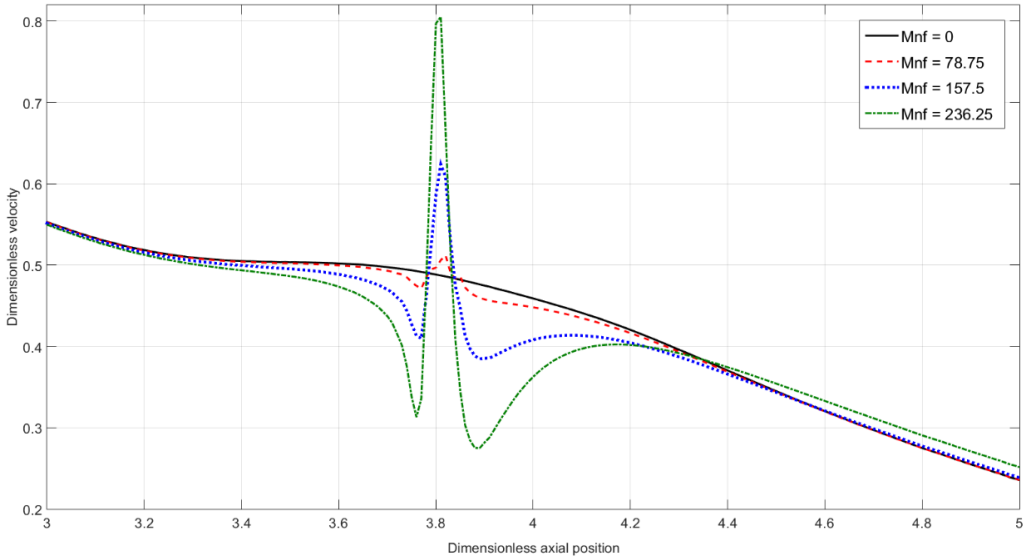

Figure 8. Variation of Axial Velocity Profile along $y = 0.01$ at Different Magnetic Field Intensity $Mn_F = 0,\ 78.75,\ 157.5$ and 236.25 with $\mathrm{Re} = 250$.

Conflicts of Interest

The author(s) declare(s) that there is no conflict of interest regarding the publication of this paper.

Acknowledgment

This work was funded by the Universiti Teknologi Malaysia (UTM) under UTM Fundamental Research (UTMFR) grant 21H48 and UTMShine grant 09G88.

References

[1] Reddy, K. S., & Yusuf, S. (1998). Emerging epidemic of cardiovascular disease in developing countries. *Circulation*, *97*(6), 596-601.

[2] Hajar, R. (2017). Risk factors for coronary artery disease: historical perspectives. *Heart views: The official journal of the Gulf Heart Association*, *18*(3), 109.

[3] Tegos, T. J., Kalodiki, E., Sabetai, M. M., & Nicolaides, A. N. (2001). The genesis of atherosclerosis and risk factors: A review. *Angiology*, *52*(2), 89-98.

[4] Srivastava, V. P. (1995). Arterial blood flow through a nonsymmetrical stenosis with applications. *Japanese Journal of Applied Physics*, *34*, 6539.

[5] Kasiman, E. H. (2012). *Mixed formulations for Navier Stokes equations with magnetic effect in rectangular channel*. MEng Thesis, Universiti Teknologi Malaysia, Skudai.

[6] Tzirtzilakis, E. E. (2005). A mathematical model for blood flow in magnetic field. *Physics of Fluids*, *17*, 1-15.

[7] Loukopoulos, V. C., & Tzirtzilakis, E. E. (2004). Biomagnetic channel flow in spatially varying magnetic field. *International Journal of Engineering Science*, *42*(5-6), 571-590.

[8] Reddy, K., Reddy, M., & Reddy, R. (2011). Mathematical model governing magnetic field effect on bio magnetic fluid flow and orientation of red blood cells. *Pac.-Asian J. Math*, *5*, 344-356.

[9] Tzirakis, K., Papaharilaou, Y., Giordano, D., & Ekaterinaris, J. (2014). Numerical investigation of biomagnetic fluids in circular ducts. *International Journal for Numerical Methods in Biomedical Engineering*, *30*(3), 297-317.

[10] Jamalabadi, M. Y. A., Daqiqshirazi, M., Nasiri, H., Safaei, M. R., & Nguyen, T. K. (2018). Modeling and analysis of biomagnetic blood Carreau fluid flow through a stenosis artery with magnetic heat transfer: A transient study. *PloS one*, *13*(2), 42-51.

[11] Higashi, T., Yamagishi, A., & Takeuchi. A. (1993). Orientation of erythrocytes in a strong static magnetic field. *Blood*, *82*(4), 1328-1334.

[12] Haik, Y., Chen, J. C., & Pai, V. M. (1996). Development of bio-magnetic fluid dynamics. *In Proceedings of the Ninth International Symposium on Transport Properties in Thermal Fluid Engineering*, 25-28.

[13] Pauling, L., & Coryell, C. D. (1936). The magnetic properties and structure of hemoglobin, oxyhemoglobin and carbonmonoxyhemoglobin. *Proceedings of the National Academy of Sciences*, *22*(4), 210-216.

[14] Loukopoulos, V. C., Bourantas, G. C., Labropoulos, D., & and Spa, V. N. (2016). Numerical study of magnetic particles concentration in biofluid (blood) under the influence of high gradient magnetic field in microchannel. *In 7th European Congress on Computational Methods in Applied Sciences and Engineering: ECCOMAS Congress*, 1084-1092.

[15] Rosensweig, R. E. (1985). *Ferrohydrodynamics*. Cambridge University Press Cambridge. New York, Melbourne.

[16] Yamada, Y., Yoshimura, N., & Sakurai, T. (1968). Plastic stress-strain matrix and its application for the solution of elastic-plastic problems by the finite element method. *International Journal of Mechanical Sciences*, *10*(5), 343-354.

[17] Babuška, I., Andersson, B., Guo, B., Melenk, J., & Oh, H. (1996). Finite element method for solving problems with singular solutions. *Journal of Computational and Applied Mathematics*, *74*(1-2), 51-70.

[18] Formaggia, L., Lamponi, D., & Quarteroni, A. (2003). One-dimensional models for blood flow in arteries. *Journal of Engineering Mathematics, 47*(3), 251-276.

[19] de Souza, M. M., & Manica, C. C. (2017). Leray-deconvolution model to Navier–Stokes equations by finite element. *Computational and Applied Mathematics, 36*(3), 1161-1172.

[20] Wei, F., Westerdale, J., McMahon, E. M., Belohlavek, M., & Heys, J. (2012). Weighted least-squares finite element method for cardiac blood flow simulation with echocardiographic data. *Computational and Mathematical Methods in Medicine, 2012*.

[21] Zain, N. M., & Ismail, Z. (2017). Modelling of Newtonian blood flow through a bifurcated artery with the presence of an overlapping stenosis. *Malaysian Journal of Fundamental Applied Sciences, 13*(2017), 304-309.

[22] Achaba, L., Mahfouda, M., & Benhadida, S. (2016). Numerical study of the non-Newtonian blood flow in a stenosed artery using two rheological models. *Thermal Science, 20*(2), 449-460.

[23] Bazilevs, Y., Zhang, Y., Calo, V. M., Goswami, S., Bajaj, C. L., & Hughes, T. J. (2018). Isogeometric analysis of blood flow: A NURBS-based approach. In *Computational Modelling of Objects Represented in Images* (pp. 91-96): CRC Press.

[24] Tzirtzilakis, E. E., & Xenos, M. A. (2013). Biomagnetic fluid flow in a driven cavity. *Meccanica*, *48*(1), 187-200.

[25] Abdullah, N., Ismail, Z., Halifi, A. S., Ayob, A. R., Kasiman, E. H., & Amin, N. S. (2020). Numerical computations of biomagnetic fluid flow in a lid driven cavity. *CFD Letters*, *12*(4), 43-53.